대한기계학회 2001년도 춘계학술대회논문집 B pp. 601~606 KSME 01S257

Dynamic Analysis of the Effect of Base Flexibility on a Spinning Disk Dynamics in a Small Size Disk Drive

Sung Jin Lee* • Soon Kyo Hong* • Young Min Cheong*

소형 디스크 드라이브에 있어서 베이스 강성이 회전하는 원판에 미치는 동적영향 분석

이 성진*, 홍 순교*, 정 영민*

Key Words : Free Vibration Analysis, Assumed Mode Method, Coupling, Disk, Spindle, Small Size Disk Drive, Flexible Baseplate

Abstract

Free vibration analysis was performed for a spinning disk/spindle system mounted on a flexible baseplate. A simplified model was presented considering the effects of the baseplate flexibility on a disk/spindle system, and the equations of motion were derived by the assumed mode method and Lagrange's equation. From the results of the free vibration analysis, the variations of the natural frequencies were investigated by changing rotating speed, baseplate thickness. They were attributed to the coupling between the flexible modes of the spinning disk/spindle system and the baseplate. This simplified model was used to predict the dynamic characteristics of a small size disk drive. The validity of the simplified model was verified by experiments and FE analysis.

1. Introduction

It is very important to analyze the dynamic characteristics of a spinning disk in recording/storage systems, e.g., floppy disk, hard disk, CD-ROM disk and digital video disk (DVD). Especially, in the small form factor design of a storage device, it's very difficult to keep the rigidity of a housing structure like a baseplate. The presence of a stationary baseplate has caused the dynamic coupling with the modes of a disk/spindle system. The dynamic coupling phenomena make a change the characteristics of the flexible disk/spindle system. In order to read and write the information quickly and exactly, even under larger storage density, it is highly demanded to predict and analyze the vibration characteristics of the spinning disk.

Numerous studies have been reviewed in the fields of free vibration, critical speed, dynamic response and stability of the spinning disk, and a number of researches have been performed for the flexible disk with a flexible shaft and blades [1-2]. Also, a spindle motor consists of a vertical shaft and two deep-groove ball bearings partially filled with grease. Balls are not perfectly round and both balls and races deform slightly under the pre-load. These factors caused the spindle to generate randomly or non-repeatable run-out at bearing defect frequencies [3]. A theoretical model for single disk and rigid spindle motor with the flexible disk and the bearing was presented by Ku and Shen [4].

In spite of many previous studies, a theoretical model for a spinning flexible disk/spindle system mounted on a flexible baseplate have not been presented yet. The theoretical model should identify the behaviors of a spinning flexible disk/spindle system interacting with a flexible baseplate. The analysis about the effects of a flexible baseplate dynamics on a spinning disk/spindle system dynamics should become more important in small size storage device design.

In this paper, a simplified model is presented for a single disk and rigid spindle motor mounted on a baseplate considering the disk and baseplate flexibility. The free vibration analysis of these systems is explored. The system is modeled as follows. Firstly, a disk is clamped to a rigid spindle, and the spindle is attached to a rigid shaft with the radial, axial, and torsional supported springs and dampers. These values were tuned by FE analyses and experiments. Secondly, the bottom of the rigid shaft is fixed at a point on a flexible baseplate. In order to derive the equations of motion, total potential and kinetic energies are calculated by summing the potential and kinetic energies of each substructure and the joint part. It is assumed that the flexible motions of

* Opto-mecha Team., Digital Media R&D Center, Samsung Electronics Co., Ltd., 416 Maetan-3-dong, Paldal-ku, Suwon, Kyunggi-do, 442-742, Korea

the disk and the baseplate are approximated by the superposition of the comparison functions. The discretized total potential and kinetic energies are represented by substituting the assumed modes of the disk and the baseplate into the total potential and kinetic energies. By Lagrange's equation, the equations of motion are derived. From free vibration analysis, the natural frequencies are calculated, and the coupling is shown between the flexible modes of each spinning disk/spindle and baseplate.

The proposed simplified model is used to predict the dynamic characteristics of a small size storage device. The validity of the model is verified by experiments and FE analysis. Also, the effects of baseplate dynamics on the natural frequencies of the system are explored.

2. The Simplified Modeling of the System

A simplified model of a disk-rotor-bearing system is shown in Figure 1 (a). However, in order to model the spinning flexible disk/spindle system mounted on a baseplate, another model should be needed as shown in Figure 1 (b). The spindle motor is supported with two bearings, and these bearings are modeled as springs with the axial, radial and torsional stiffnesses.

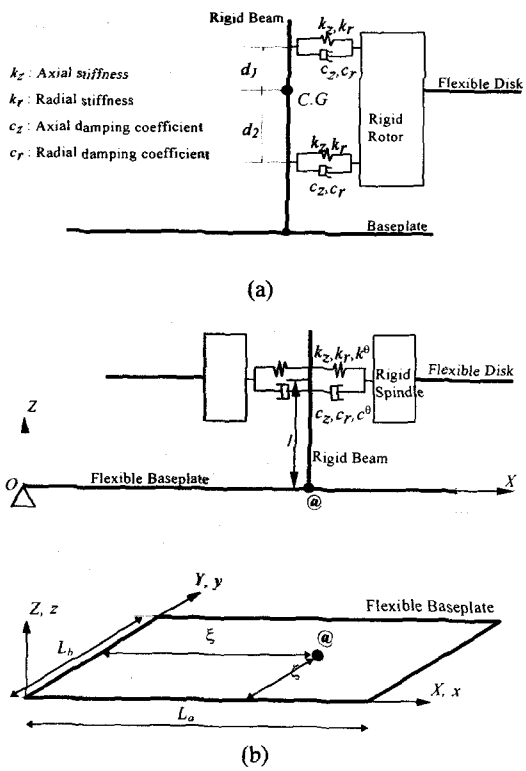

Figure 1: (a) A lumped model of a disk-rotor-bearing system, and (b) schematic of a flexible disk/spindle system mounted on a baseplate.

The torsional stiffness in bearings is determined by geometric relation as:

$$k_\theta = k_r\left(d_1^2 + d_2^2\right) \quad (1)$$

where, d_1 and d_2 are the distances from the center of gravity to each bearing, respectively.

The flexible disk is clamped to a rigid spindle at the inner radius (a, see Figure 3) and it moves freely at the outer radius (b, see Figure 3). The rigid spindle is connected to a rigid beam with a torsional spring (k_θ), an axial spring (k_z), a radial spring (k_r), a torsional damper (c_θ), an axial damper (c_z) and a radial damper (c_r). The spindle system is a 5 degrees-of-freedom, and the variables are x_S, y_S, z_S, θ_x, and θ_y, as shown in Figure 2.

The motion of the spinning disk is described in two coordinate systems: O_1-$x_2y_2z_2$ and O_1-$X_1Y_1Z_1$ (see Figure 3). The O_1-$x_2y_2z_2$ is a local coordinate system, while the O_1-$X_1Y_1Z_1$ is an inertial reference system. The transverse deflection of the disk (w_D) is defined about the local O_1-$x_2y_2z_2$ system. The disk rotates about the O_1z_2-axis with the constant spinning speed (Ω).

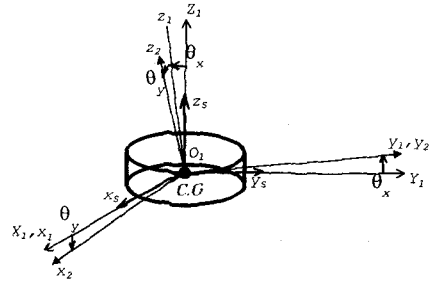

Figure 2: Schemetic of 5 DOFS of a spindle system.

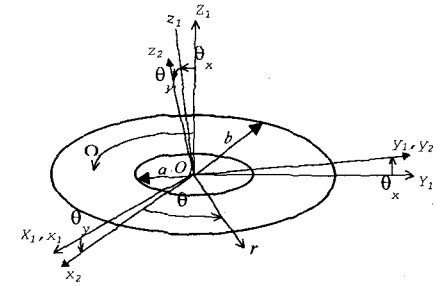

Figure 3: Schemetic of coordinate system of a disk.

2.1 Potential Energy

In order to obtain the total kinetic and potential energies, the whole system was divided into two substructures like the baseplate and the disk/spindle. The total potential energy of the spinning disk/spindle system mounted on a baseplate was calculated by summing the strain energy of the disk and the baseplate, and the potential energy of joint stiffness between the rigid beam and the spindle. The strain energy of the baseplate was

derived by Kirchhoff plate theory as the following:

$$U_B = \frac{D_B}{2}\int_0^{L_a}\int_0^{L_b}\left\{\left(\frac{\partial^2 w_B}{\partial x^2}\right)^2+\left(\frac{\partial^2 w_B}{\partial y^2}\right)^2+2\nu_B\frac{\partial^2 w_B}{\partial x^2}\frac{\partial^2 w_B}{\partial y^2}+2(1-\nu_B)\left(\frac{\partial^2 w_B}{\partial x\partial y}\right)^2\right\}dxdy \quad (2)$$

$$D_B = \frac{E_B h_B^3}{12(1-\nu_B^2)} \quad (3)$$

where, w_B, D_B, E_B, h_B and ν_B are transverse displacement, flexural rigidity, Young's modulus, thickness and Poisson's ratio, respectively.

The strain energy of the spinning disk was calculated under assuming the thickness being small. Also, It was assumed that in-plane deflections were steady and axisymmetric. The strain energy of the spinning disk was derived by Von Karman strain theory and the stress-strain relations for a homogeneous elastic Hookean material [5] as:

$$U_D = \frac{D_D}{2}\int_a^b\int_0^{2\pi}\left[\left(\nabla^2 w_D\right)^2-2(1-\nu_D)\left\{\left(\frac{1}{r}\frac{\partial w_D}{\partial r}+\frac{\partial^2 w_D}{r^2\partial\theta^2}\right)\left(\frac{\partial^2 w_D}{\partial r^2}\right)-\left(\frac{\partial^2 w_D}{r\partial r\partial\theta}-\frac{\partial w_D}{r^2\partial\theta}\right)^2\right\}\right]rdrd\theta + \frac{1}{2}\int_a^b\int_0^{2\pi}\left[Q_r^{lin}\left(\frac{\partial w_D}{\partial r}\right)^2+Q_\theta^{lin}\left(\frac{\partial w_D}{r\partial\theta}\right)^2\right]rdrd\theta \quad (4)$$

$$\nabla^2 = \frac{\partial^2}{\partial r^2}+\frac{1}{r}\frac{\partial}{\partial r}+\frac{\partial^2}{r^2\partial\theta^2} \quad (5)$$

where, w_D, D_D, ν_D, Q_r^{lin} and Q_θ^{lin} are the transverse displacement, the flexural rigidity, the Poisson's ratio, and linearized internal forces per unit length in the middle surface, respectively. Q_r^{lin} and Q_θ^{lin} are produced by the centrifugal effect of a spinning disk, and uniquely determined by the ordinary differential equation derived by Hamilton's principle as:

$$\frac{dQ_r^{lin}}{dr}+\frac{Q_r^{lin}-Q_\theta^{lin}}{r} = -r\rho_D h_D\Omega^2 \quad (6)$$

$$Q_r^{lin} = h_D\frac{E_D}{1-\nu_D^2}\left(\frac{du_D}{dr}+\nu_D\frac{u_D}{r}\right),$$

$$Q_\theta^{lin} = h_D\frac{E_D}{1-\nu_D^2}\left(\nu_D\frac{du_D}{dr}+\frac{u_D}{r}\right) \quad (7)$$

where, u_D, E_D and h_D are the radial displacement in the middle surface, Young's modulus, and the thickness, respectively.

The potential energy of joint part between the rigid beam and the spindle is expressed as:

$$U_S = \frac{1}{2}k_z\left(z_S-w_B\Big|_{\substack{x=\xi\\y=\varsigma}}\right)^2+\frac{1}{2}k_r\left(x_S+l\frac{\partial w_B}{\partial x}\Big|_{\substack{x=\xi\\y=\varsigma}}\right)^2+\frac{1}{2}k_r\left(y_S+l\frac{\partial w_B}{\partial y}\Big|_{\substack{x=\xi\\y=\varsigma}}\right)^2+\frac{1}{2}k_\theta\left(\theta_x-\frac{\partial w_B}{\partial y}\Big|_{\substack{x=\xi\\y=\varsigma}}\right)^2+\frac{1}{2}k_\theta\left(\theta_y+\frac{\partial w_B}{\partial x}\Big|_{\substack{x=\xi\\y=\varsigma}}\right)^2 \quad (8)$$

where, ξ and ς are the distances at a fixed point @ on the baseplate(see Figure 1), and l is the distance from the baseplate to the center of mass of the disk/spindle system.

2.2 Kinetic Energy

Firstly, the kinetic energy of the base plate is expressed as:

$$T_B = \frac{\rho_B h_B}{2}\int_0^{L_a}\int_0^{L_b}\left(\frac{\partial w_B}{\partial t}\right)^2 dxdy \quad (9)$$

where, ρ_B and is the density of a baseplate.

Also, the kinetic energy of the disk was calculated. The velocity in an arbitrary point of the disk is shown as:

$$\mathbf{v} = \bar{\mathbf{v}} - z\psi \quad (10)$$

where, ψ is the angular velocity vector at a point in the middle surface, and $\bar{\mathbf{v}}$ is the linear velocity vector at a point in the middle plane as [5]:

$$\bar{\mathbf{v}} = \dot{z}_S\mathbf{e}_{Z_1}+\dot{x}_S\mathbf{e}_{X_1}+\dot{y}_S\mathbf{e}_{Y_1}+\dot{w}_D\mathbf{e}_{z_2}+\Omega\,\mathbf{e}_{z_2}\times\mathbf{r}+\left(\dot{\theta}_x\mathbf{e}_{X_1}+\dot{\theta}_y\mathbf{e}_{y_2}\right)\times\mathbf{r} \quad (11)$$

$$\mathbf{r} = (r+u_D)\left(\cos\theta\,\mathbf{e}_{x_2}+\sin\theta\,\mathbf{e}_{y_2}\right) \quad (12)$$

where, Ω is the rotating speed, $\mathbf{e}_{X_1}$, $\mathbf{e}_{Y_1}$ and $\mathbf{e}_{Z_1}$ are the unit vectors in the X_1, Y_1 and Z_1 directions, and $\mathbf{e}_{x_2}$, $\mathbf{e}_{y_2}$ and $\mathbf{e}_{z_2}$ are the unit vectors in the x_2, y_2 and z_2 directions, respectively. The relations of these two sets of the unit vectors are represented by:

$$\begin{Bmatrix}\mathbf{e}_{X_1}\\ \mathbf{e}_{Y_1}\\ \mathbf{e}_{Z_1}\end{Bmatrix} = \begin{bmatrix}\cos\theta_y & 0 & \sin\theta_y\\ 0 & 1 & 0\\ -\sin\theta_y & 0 & \cos\theta_y\end{bmatrix}\begin{bmatrix}1 & 0 & 0\\ 0 & \cos\theta_x & -\sin\theta_x\\ 0 & \sin\theta_x & \cos\theta_x\end{bmatrix}\begin{Bmatrix}\mathbf{e}_{x_2}\\ \mathbf{e}_{y_2}\\ \mathbf{e}_{z_2}\end{Bmatrix} \quad (13)$$

Since the thickness of the disk is small, the kinetic energy of the disk is simplified as:

$$T_D = \frac{1}{2}\rho_D h_D\int_a^b\int_0^{2\pi}\bar{\mathbf{v}}\cdot\bar{\mathbf{v}}\,rdrd\theta \quad (14)$$

where, ρ_D and is the density of the disk.

Finally, the kinetic energy of the spindle is expressed as:

$$T_S = \frac{1}{2}I_S\left(\dot{\theta}_x^2+\dot{\theta}_y^2\right)+I_S\left(\Omega-\dot{\theta}_y\theta_x\right)^2+\frac{1}{2}m_S\left(\dot{z}_S^2+\dot{x}_S^2+\dot{y}_S^2\right) \quad (15)$$

where, m_s and I_s are the mass and the mass moment of inertia, respectively. In equations (14) and (15), higher order nonlinear terms are neglected, because u_D, w_D, x_S, y_S, z_S, θ_x and θ_y are small.

2.3 Discretization

The motion of each substructure can be shown approximately by the superposition of the comparison functions. The rigid body motion of the spindle is a five degrees-of-freedom system as:

$$\mathbf{q_S} = \left[z_S \quad x_S \quad y_S \quad \theta_x \quad \theta_y\right]^T \quad (16)$$

The deflection of the baseplate is represented in terms of the comparison functions, which are the mode shapes of a simple uniform rectangular plate with simply supported boundary conditions:

$$w_B = \sum_{m=1}^{M}\sum_{n=1}^{N}B_{mn}(t)\sin\frac{m\pi x}{L_a}\sin\frac{n\pi y}{L_b} = \Phi_B\mathbf{q_B} \quad (17)$$

$$\Phi_B = \left[\sin\frac{\pi x}{L_a}\sin\frac{\pi y}{L_b} \quad \sin\frac{2\pi x}{L_a}\sin\frac{\pi y}{L_b} \quad \cdots\right] \quad (18)$$

$$\mathbf{q_B} = \left[B_{11}(t) \quad B_{21}(t) \quad \cdots\right]^T$$

where, Φ_B is the row vector relating the comparison functions to describe the baseplate motion and $\mathbf{q}_B$ is the column vector relating the time-dependent generalized coordinates.

The deflection of the disk is also expressed in terms of the comparison functions. They are satisfied with clamped boundary condition at the inner radius a, and free at the outer radius b and normalization condition. Generally, for the stationary disk, the natural frequencies of the modes with one or more nodal circles are larger than those of modes with zero nodal circle and even with three or four nodal circles. That is why the analysis includes the only mode with zero nodal circle in this paper. The transverse deflection of the flexible disk is expressed as:

$$w_D(r,\theta,t) = \sum_{n=0}^{N}\left[C_n(t)\cos n\theta + S_n(t)\sin n\theta\right]R_n(r) = \Phi_D \mathbf{q}_D \tag{19}$$

$$\Phi_D = \left[R_0(r) \quad \cos\theta\, R_1(r) \quad \sin\theta\, R_1(r) \quad \cdots\right]$$
$$\mathbf{q}_D = \left[C_0(t) \quad C_1(t) \quad S_1(t) \quad \cdots\right]^T \tag{20}$$
$$R_n(r) = (r-a)^2\left({}_0c_n + {}_1c_n r + {}_2c_n r^2\right)$$

where, N is the total number of nodal circles. ${}_0c_n$, ${}_1c_n$ and ${}_2c_n$ are determined by the natural boundary conditions and the normalized condition[5].

By substituting equations (16), (17) and (19) into equations (2), (4), (8), (9), (14) and (15), the discretized total energy functions are as:

$$U = U_B + U_D + U_S \tag{21}$$
$$T = T_B + T_D + T_S \tag{22}$$

2.4 Equations of Motion

The total kinetic and potential energies are expressed in terms of a number of generalized coordinates. The equations of motion of the spinning disk/spindle system mounted on a baseplate are derived by Lagrange's equation as:

$$\frac{d}{dt}\left(\frac{\partial(T-U)}{\partial \dot{q}_i}\right) - \frac{\partial(T-U)}{\partial q_i} = \Xi_i \tag{23}$$

where, q_i and Ξ_i are the independent generalized coordinates and the nonconservative generalized forces including viscous damping, respectively:

$$\mathbf{q} = \left[q_1\ q_2 \cdots q_i \cdots\right]^T = \left[\mathbf{q}_D{}^T\ \mathbf{q}_S{}^T\ \mathbf{q}_B{}^T\right]^T \tag{24}$$

$$\left[\Xi_1\ \Xi_2 \cdots \Xi_i \cdots\right]^T = -\mathbf{C}_d\,\dot{\mathbf{q}} \tag{25}$$

where, $\mathbf{C}_d$ is an equivalent damping matrix.

By substituting equations (21) and (22) into equation (23), the equations of motion are finally obtained as matrix forms.

$$\mathbf{M}\ddot{\mathbf{q}} + \mathbf{C}\dot{\mathbf{q}} + \mathbf{K}\mathbf{q} = \mathbf{0} \tag{26}$$

where,

$$\mathbf{M} = \begin{bmatrix} \mathbf{M}_D^1 & \left(\mathbf{M}_{SD}^1\right)^T & \mathbf{0} \\ \mathbf{M}_{SD}^1 & \mathbf{M}_S^1 + \mathbf{M}_S^3 & \mathbf{0} \\ \mathbf{0} & \mathbf{0} & \mathbf{M}_B \end{bmatrix} \tag{27}$$

$$\mathbf{C} = \begin{bmatrix} \mathbf{M}_D^3 - \mathbf{M}_D^4 & -\left(\mathbf{M}_{SD}^2\right)^T & \mathbf{0} \\ \mathbf{M}_{SD}^2 & \mathbf{M}_S^2 - \left(\mathbf{M}_S^2\right)^T + \mathbf{M}_S^4 - \left(\mathbf{M}_S^4\right)^T + \mathbf{C}_S & \mathbf{C}_{SB} \\ \mathbf{0} & \left(\mathbf{C}_{SB}\right)^T & \mathbf{C}_B \end{bmatrix} \tag{28}$$

$$\mathbf{K} = \begin{bmatrix} \mathbf{K}_D - \mathbf{M}_D^2 & \mathbf{0} & \mathbf{0} \\ \mathbf{0} & \mathbf{K}_S & \mathbf{K}_{SB} \\ \mathbf{0} & \left(\mathbf{K}_{SB}\right)^T & \mathbf{K}_B + \mathbf{K}_B^S \end{bmatrix} \tag{29}$$

3. Simulation Results

3.1 Estimations of System Parameters

The simplified model presented in Chapter 2 was applied to a real product of small size optical storage device, and the variations of the natural frequencies were investigated by changing design parameters. Firstly, in order to calculate the system parameters being used in the simplified model and verify the results of the simulations, the experiments with impulse tests and FEM were performed for single disk/DC spindle motor system mounted on a baseplate. A capacitance typed gap sensor was evaluated for measuring the deflection of the disk, and the smallest and lightest B&K accelerometer was evaluated for modal analysis to minimize the influence on the system. Also, a small sized impulse hammer was used for excitation, because the experimental object was small sized and light weighted, and it could be excited to higher frequency range beyond 7,000 Hz. Dytran 5800SL was evaluated for this purpose. Hewlett Packard FFT analyzer was used for calculating frequency response function.

The baseplate was used for the stator of the motor in itself. Two long side of the baseplate was fixed to a rigid ground with experimental jigs. The speed of the motor was adjustable and controlled by an electronic driver board.

Table 1: Properties and values of single disk-motor system.

	Properties	Values
Disk	Inner radius	5.5 (mm)
	Outer radius	23 (mm)
	Thickness	0.6 (mm)
	density	1200 (Kg/m^3)
	poisson' s ratio	0.3
	young' s modulus	2.5 (GPa)
Rotor	Total Mass	5.96 (g)
	Total Transverse mass moment of inertia	0.327 (Kg·mm^2)
Bearing	Bearing span	2.6 (mm)
	Radial stiffness	7.6×10^6 (N/m)
	Axial stiffness	6.27×10^6 (N/m)
	Torsional stiffness	25.7 (N·m/radian)

The torsional stiffness of the bearing, k_θ was calculated to be 25.7 N·m/radian by equation (1). The axial and torsional bearing stiffness was tuned by

comparing FE analysis results with experimental results. The properties of the used single disk/motor system and baseplate are shown in Tables 1 and 2.

Table 2: Properties and values of baseplate.

	Properties	Values
L_a		74 (mm)
L_b		53 (mm)
ρ_B	Density	8200 (Kg/m^3)
ν_B	Poisson' s ratio	0.3
E_B	Young modulus	210 (GPa)
ξ	Connecting position	27 (mm)
ζ		$\frac{1}{2}L_b$
h_B	Thickness	0.4 mm

3.2 Simulation Results

Before performing the simulations of the system, the system parameters were chosen as in Tables 1 and 2. Commercial programs like Mathematica, MATLAB and ANSYS were used for the simulations.

The results of the simulations and the experiments for the baseplate and the disk are shown in Table 3. The long sides of the baseplate were clamped, and the inner radius of the disk was also clamped. The simulations agree well with the experiments. The variations of the natural frequencies by changing the rotating speeds are shown in Figure 4. From these comparisons, the validity of a simplified model in this paper was verified.

Table 3 (a): Natural frequencies of a disk at $\Omega = 0$.

Mode	Natural Frequencies (Hz)		
	Analytical	FEM	Experiment
(0,1)	425	427	418
(0,0)	443	448	450
(0,2)	543	541	536
(0,3)	993	994	978

Table 3 (b): Natural frequencies of a baseplate at $\Omega = 0$.

Mode	Natural Frequencies (Hz)		
	Analytical	FEM	Experiment
(1,1)	972	966	964
(2,1)	1506	1710	1890
(3,1)	-	2220	2120
(1,2)	2596	2280	2270

The effect of the baseplate dynamics on the natural frequencies of the disk/rotor system was explored for both flexible and rigid baseplates. The natural frequencies of the other modes except the axial mode were almost similar for both cases, as shown in Table 4 at rotating speed being zero. But, as rotating speed increases, The baseplate dynamics has the strongest effect on both axial modes and rocking modes of the system. In Figure 4, the axial mode is independent of rocking mode on a rigid baseplate. These two modes could not have any dynamic relations each other. Otherwise, when the baseplate becomes flexible, axial and rocking modes are fully coupled in some dynamic condition. When the rotating speed is around zero, lines ① and ② are a backward rocking and an axial dominant modes, respectively. However, as the rotating speed increases, the natural frequencies of two modes become closer and two modes are mixed. That is, these two modes are fully coupled as shown in circle on Figure 4. As the rotating speed keeps increasing beyond that value, the coupled two modes are separated to axial and backward rocking dominant modes. It is remarkable that during the mode coupling, two lines exchange their modes each other.

Table 4: Natural frequencies of a disk/spindle motor mounted on a flexible baseplate and a rigid baseplate, at $\Omega = 0$.

Mode	Rigid baseplate (Hz)		Flexible baseplate (Hz)	
	Analytical	FEM	Analytical	Experiment
Rocking	417	414	414, 417	
Axial + Baseplate (In Phase)	443	447	402	
(0,2) of disk	543	541	543	
(0,3) of disk	993	994	993	
Axial + Baseplate (Out of Phase)	-	-	583	

By the way, it's interesting that mode coupling phenomena between axial and rocking modes have a big correlation with pivot point on baseplate (point @ in Figure 1(b)). If the pivot point lies on symmetric line, $\xi=L_a/2$, $\zeta=L_b/2$, there is no mode coupling between two modes. In this case, baseplate flexibility makes an only influence on an axial mode. Because, this symmetric pivot point on the baseplate can't make a tilting motion at all in the low frequency range. The tangent line at the pivot point is always parallel to XY plane.

Finally, the effect of baseplate thickness variation on the natural frequencies of the system were explored. The natural frequencies relating the axial mode are very sensitive to baseplate flexibility. Especially, the disk/spindle system on the very flexible baseplate – under 0.4mm has several coupled modes between rocking and axial modes shown in Figure 5. In these cases, the natural frequencies of the system are very different from those of the disk/spindle mounted on a stiff baseplate. So, the accurate prediction of the dynamic performance of the disk/spindle system on such a flexible baseplate is necessary for the design of the high performance storage device. By the way, we find that the natural frequencies of the system converge to those of rigid baseplate, as the thickness of the baseplate increases to high.

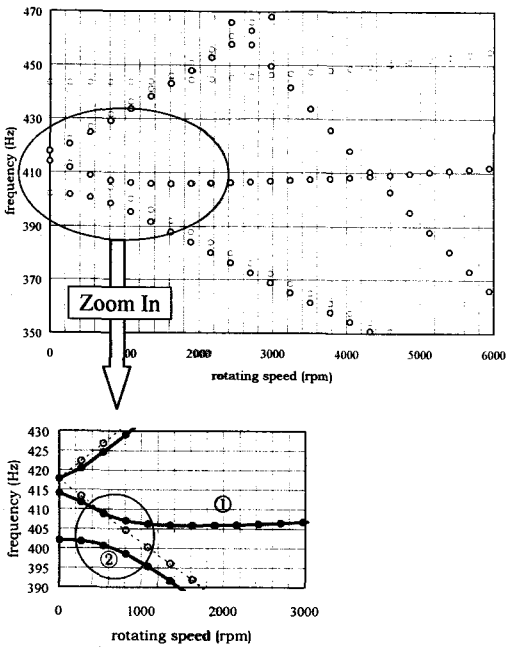

Figure 4: Variations of natural frequencies considering the effect of the baseplate dynamics by changing the rotating speed. Solid line : a flexible baseplate, dotted line : a rigid baseplate. The baseplate thickness is fixed to be 0.4 mm.

4. Conclusions

The dynamic characteristics of the flexible disk/spindle system mounted on a flexible baseplate were analyzed. A simplified model was presented considering the effects of the baseplate dynamics on a disk/spindle system, and the equations of motion were derived by the assumed mode method and Lagrange's equation. The effect of the baseplate flexibility on dynamics of the disk was systematically explored. Also, it was found that the baseplate flexibility had the strong effect on the flexible disk modes with zero nodal diameter. Especially, as the rotating speed increases, the flexible disk modes with zero nodal diameter were coupled with those with one nodal diameter, so the natural frequencies of the disk/spindle system change differently compared with the system on rigid baseplate. The more flexible is the baseplate, the more complicated is the dynamic performance of the disk/spindle system.

The simplified model presented in this paper was applied to a small size storage device, and its validity was verified from the experiments and FEM. The results of simulations agreed well with the experiments. The baseplate flexibility severely affected the axial mode of the disk/rotor system. It was found that the baseplate flexibility made the rocking modes and the axial mode being coupled, while being completely decoupled for a rigid baseplate. It was found that the dynamic characteristics of the disk/spindle motor mounted on a flexible baseplate were very complicated.

We hope that this paper will give a designer of storage device a big help to determine the design parameters and predict the dynamic behaviors of the system, in order to increase data storage and reduce access time and size.

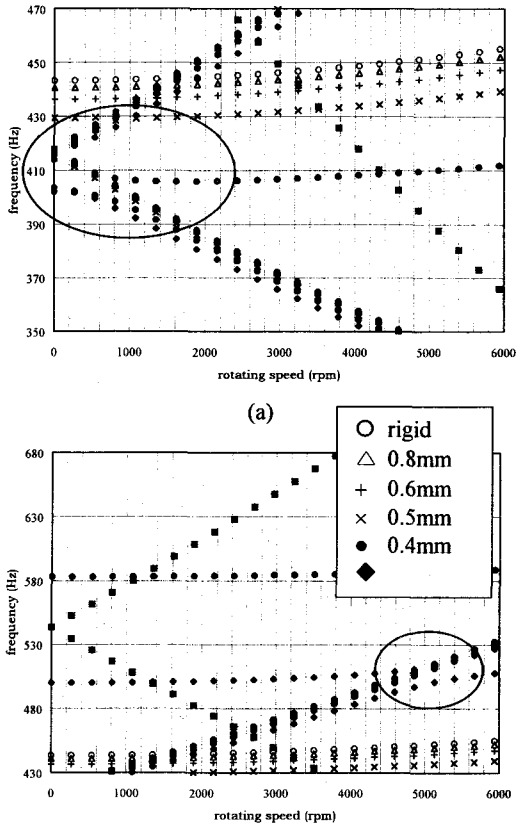

Figure 5: Variations of natural frequencies. Baseplate thickness varies from 0.3mm to 0.8mm

REFERENCES

(1) S. Okamoto, M. Sakata, K. Kimura and H. Ohnabe 1995 *Journal of Sound and Vibration* **184[5]**, 887-906. Vibration Analysis of a High Speed and Light Weight Rotor System Subjected to a Pitching or Turning Motion, II: A Flexible Rotor System on Flexible Suspensions.

(2) S. B. Chun and C. W. Lee 1996 *Journal of Sound and Vibration* **189[5]**, 587-608. Vibration Analysis of Shaft-Bladed Disk System by using Substructure Synthesis and Assumed Modes Method.

(3) K. Ono, N. Saiki, Y. Sanada and A. Kumano 1991 *ASME Journal of Vibration and Acoustics* **113[3]**, 292-298. Analysis of Nonrepeatable Radial Vibration of Magnetic Disk Spindles.

(4) C. P. Roger Ku and I. Y. Shen 1996 *Tribology Transactions* **39[3]**, 579-586. Effect of Disk Flexibility on Rocking Mode Frequencies of a Disk Drive Spindle Motor System.

(5) Sung Jin Lee, Jintai Chung and Jang Moo Lee 1998 *JSME International Journal* Series **C 41[3]**, 329-337. Free Vibrations of a Flexible Spinning Disk with Axial Translation and Rigid-Body Tilting.

(6) Meirovitch, Analytical Methods in Vibrations, Macmillan